Semi-Quantitative High Resolution Electron Microscopy of Short-Range Ordered Ni_4Mo

Satoshi Hata, *Syo Matsumura, Noriyuki Kuwano and Kensuke Oki

Department of Materials Science and Technology, Graduate School of Engineering Sciences, Kyushu University 39, Kasuga, Fukuoka 816, Japan
**Department of Nuclear Engineering, Faculty of Engineering, Kyushu University 36, Fukuoka, Fukuoka 812-81, Japan*

(Received: Jan. 30, 1997 Accepted: Feb. 21, 1997)

Abstract

The atomic arrangements of the short-range ordered (SRO) structure in a Ni_4Mo alloy were investigated by means of high resolution transmission electron microscopy (HRTEM) with an Imaging Plate (IP) system. The digitally processed HRTEM images showed dot-patterns corresponding to various ordered structures as N_2M_2, $D1_a$, $D0_{22}$ and Pt_2Mo. A semi-quantitative analysis of brightness of atomic columns in the images suggests that the N_2M_2-pattern is formed by superposition of projected $D1_a$-, $D0_{22}$- and Pt_2Mo -subunit cell clusters which have been expected by our Monte Carlo simulation of the SRO state with an Ising-like model.

1. Introduction

A short-range ordered (SRO) alloy gives diffuse scatterings in the diffraction pattern and the positions of the intensity maxima correspond to those of the superlattice reflections for the long-range ordered (LRO) phase. However, it is not the case for Ni_4Mo. The Ni_4Mo alloy quenched above the critical temperature of the order-disorder transformation is short-range ordered, and exhibits diffuse intensity maxima at {1 1/2 0} positions (hereafter {*hkl*} is referred to *hkl* and its equivalent positions). The positions do not coincide with {4/5 2/5 0} for $D1_a$-type structure which is the LRO structure of the alloy. The structure has the five-time-periodicity of $(420)_{fcc}$ Planes, as shown in Figure 1 (a). Microstructures in the SRO state were investigated by various techniques including high resolution transmission electron microscopy (HRTEM) [1-5]. Various model-structures, as shown in Figure 1 (b) $D0_{22}$[1,2], (c) N_2M_2 [3,4] and (d) N_3M [5], were proposed to explain the appearance of the {1 1/2 0} reflections. However, the real SRO structure is still controversial. This is due to the fact that HRTEM does not directly show the real atomic arrangements of SRO since some local ordered regions of different phases are superimposed in the incident beam direction. We [6,7] recently carried out Monte Carlo simulation of the ordering process in Ni_4Mo with an Ising-like model to examine the local atomic arrangements in detail. The simulation

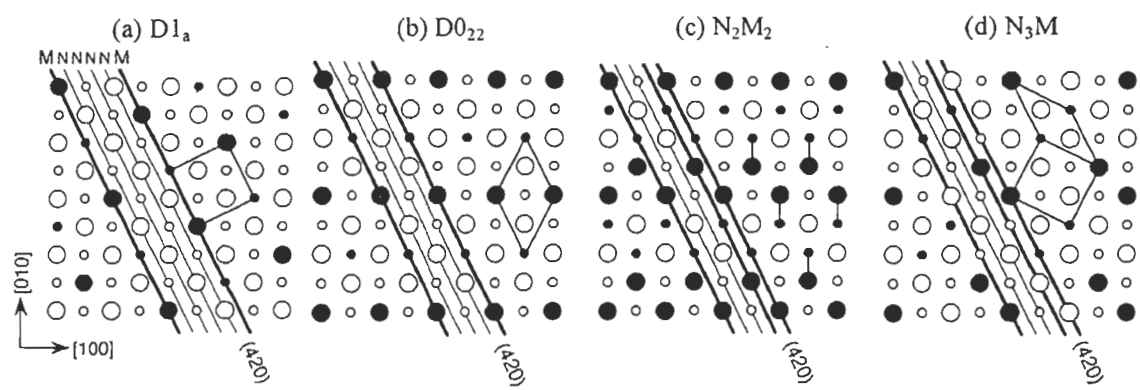

Fig. 1 (001) projections of the ordered structures which are considered to appear in the Ni-Mo system, (a) $D1_a$ (LRO structure in Ni_4Mo), (b) $D0_{22}$ (c) N_2M_2 and (d) N_3M. Closed and open circles denote Mo and Ni columns and large and small ones indicate z=0 and z=1/2 planes, respectively. N_3M structure consists of subunit cells of $D1_a$, and Pt_2Mo structures.

suggests that HRTEM images of short-range ordered Ni_4Mo locally exhibit dot patterns of the spurious ordered structure, N_2M_2, due to superposition of clusters of $D1_a$-, $D0_{22}$- and Pt_2Mo-subunit cells. However, such a superposition of ordered atomic arrangements cannot be directly confirmed by conventional HRTEM imaging.

The imaging plate (IP) system has been recently developed for TEM and has opened up quantitative imaging [8] and diffraction [9, 10] with a wide dynamic range for the electron beam and a good linearity in output signal. In the present study, we applied the IP system to HRTEM imaging of SRO in Ni_4Mo, and tried a semi-quantitative analysis of the images to confirm the superposition of ordered atomic arrangements and to extract more detailed information about the SRO structures.

2. Experiments

An alloy ingot of Ni-19.5 at% Mo was prepared by arc melting under argon atmosphere. The alloy was homogenized at 1273 K, which is within the disordered region, for 84.6 ks, and cut into disks of 3 mm in diameter. The disk specimens were annealed again at 1273 K for 84.6 ks and quenched into iced water to obtain an SRO state. The specimens were electropolished in a solution of CH_3OH and H_2SO_4. HRTEM observations were carried out with a 200 kV electron microscope with a field emission gun (JEM-2010F), and observed images were recorded on IP's.

3. Results and Discussion

Figure 2 (a) gives a (001) HRTEM image of the Ni- 19.5 at% Mo alloy quenched from 1273 K and its Fourier power spectrum. An objective aperture large enough to pass the *fcc* reflections of $hkl = 220$ was used for imaging. The image shows a quad-dot-pattern corresponding to (001) projection of the *fcc* fundamental lattice. Atomic columns with higher concentration of minority element (Mo in the present alloy) become brighter (or darker) in HRTEM images of ordered alloys. The dots in the figure (a) have been imaged in a variety of intensities wihich may accord to

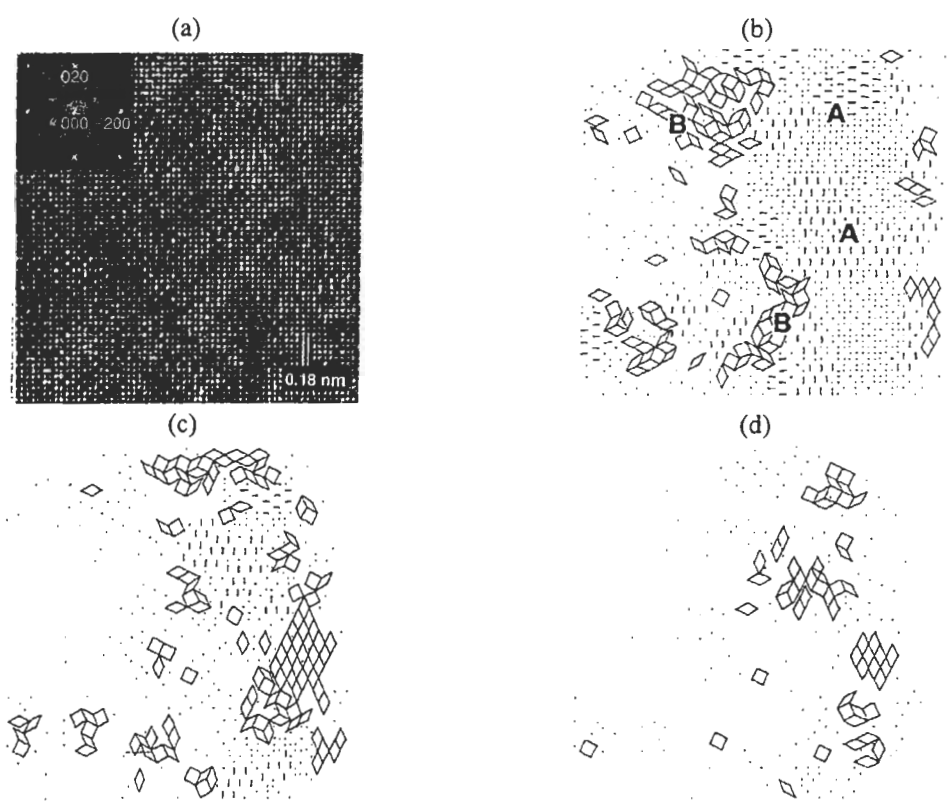

Fig. 2 (a): HRTEM image of quenched Ni-19.5 at% Mo and its Fourier power spectrum. A quad-dot-pattern corresponding to (001) projection of the *fcc* fundamental lattice is seen. (b), (c) and (d): positions of [001] atomic columns with Mo concentration over a lower, medium and higher threshold values, respectively. Clusters of $D1_a$(slanting square), $D0_{22}$(thick lozenge) and Pt_2Mo (thin lozenge) subunit cells marked A, and N_2M_2-patterns (double-dot) marked B are observed.

the SRO structure. However. no particular ordered structure can be identified directly in the conventionally printed image of the SRO alloy, in spite of the appearance of the diffuse intensity maxima at {1 1/2 0} positions in the Fourier power spectrum. This indicates that the image contains information about the SRO structure.

If background noises contained in the HRTEM image were reduced, dot-patterns of ordered structures become visible. Figures 2 (b), (c) and (d) show the positions of atomic columns which have brightness over a certain threshold value in the HRTEM images reproduced by the inverse transformation of the *fcc* and {1 1/2 0} reflections in the Fourier power spectrum. When the low threshold value of brightness is adopted (b), dots with various brightness come out together. Two types of dot-patterns are observed in the *fcc* matrix: One is the (001) projection pattern of N_2M_2 structure marked A(hereafter the dot-pattern is called "N_2M_2-pattern"), and another is clusters of $D1_a$ (slanting square), $D0_{22}$ (thick lozenge) and Pt_2Mo-type (thin lozenge) subunit cells marked B. If the threshold value is somewhat increased (c), the number of dots decreases, and the area of N_2M_2-pattems becomes relatively smaller than that of $D1_a$-, $D0_{22}$- and Pt_2Mo-subunit cells. It is seen that some N_2M_2-patterns in the images turn to other patterns of $D1_a$-, $D0_{22}$- and Pt_2Mo-subunit cells with the increase of the threshold value. When the threshold value is increased further (d), only dots with high brightness become visible. The N_2M_2-patterns disappear and only clusters of $D1_a$-, $D0_{22}$- and Pt_2Mo-subunit cells remain. Meulenaere *et al.* [11, 12] studied HRTEM images of the SRO alloys which have the {1 1/2 0} diffuse intensity maxima. It was described that the brightness of dots in the images depends on the composition in the

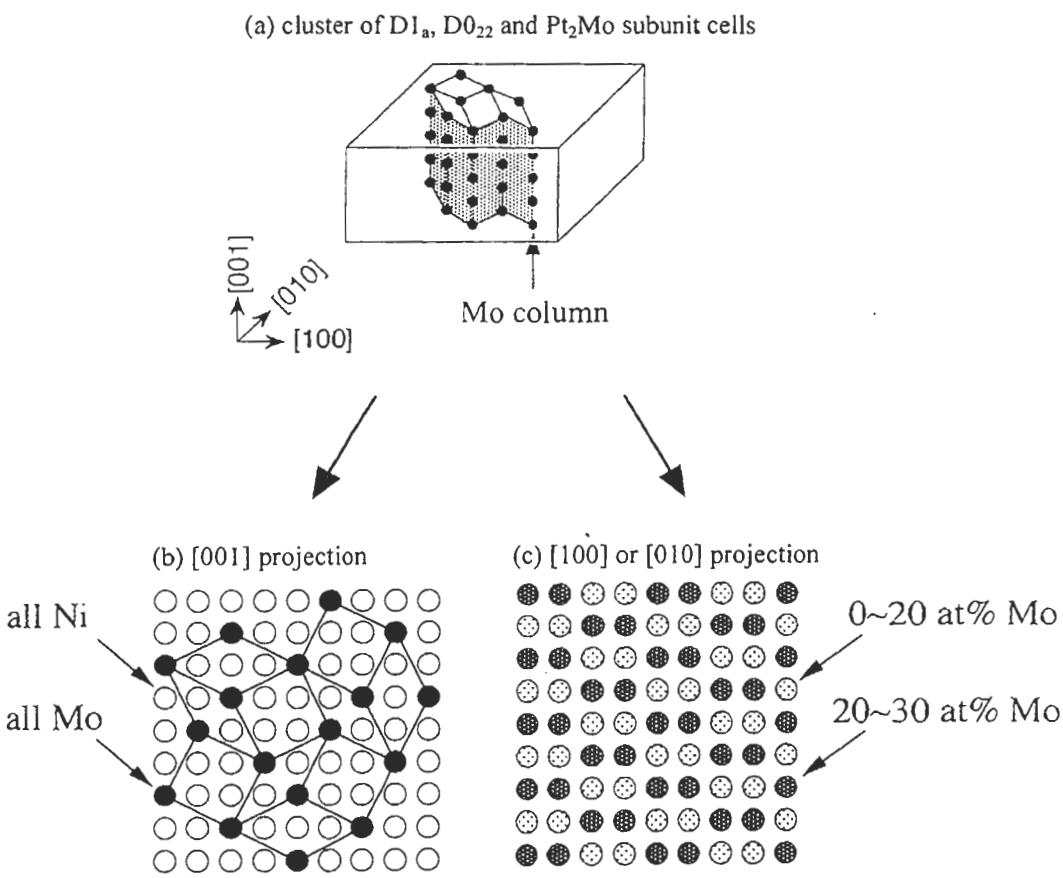

Fig. 3 Explanation for the appearance of the two types of projected patterns. Clusters of $D1_a$-, $D0_{22}$- and Pt_2Mo-subunit cells are formed in the SRO state as shown in (a). The subumt cell cluster in (a) consists of like-atom columns of Mo (shown as chains of black spheres) and Ni atoms parallel to the [001] direction. The [001] projection of the subunit cell cluster shows $D1_a$-, $D0_{22}$- and Pt_2Mo-subunit cells (b). However, the [100] or [010] projection exhibits the pattern of N_2M_2-type (c).

atomic columns. Accordingly, the present results indicate that clusters of $D1_a$-, $D0_{22}$- and Pt_2Mo-subunit cells consist of highly Mo-rich columns, and N_2M_2-patterns consist of less Mo-rich columns.

The results of the digitally processed images are in good agreement with our recent results of Monte Carlo simulation of the SRO in Ni_4Mo [6,7], In the simulation, an Ising-like model system which consists of $20\times20\times60$ *fcc* unit cells with the periodic boundary conditions was used, and neighboring atoms were directly exchanged with each other, taking into account of the pairwise atomic interactions up to the fifth nearest neighbors. The SRO structure obtained by the simulation can briefly explain the appearance of the two types of dot-patterns in the digitally processed images, as shown in Figure 3. In the SRO state, microclusters of $D1_a$-, $D0_{22}$- and Pt_2Mo-subunit cells are formed in the matrix, as shown in (a). The subumt cell cluster forms like-atom columns of Mo (shown as chains of black spheres) and Ni parallel to the [001] direction. The [001] projection of the cluster shows a dot-pattern of $D1_a$-, $D0_{22}$- and Pt_2Mo-subunit cells as in (b). In this case, atomic columns in the cluster along the projected direction consist of all Ni (open circles) or all Mo atoms (closed circles). If the subunit cell cluster is projected in the [100] or [010] directions, N_2M_2-patterns come out as in (c). The differences in composition among each column along the projected direction are smaller than those for the case of the [001] projection in (b). Thus the N_2M_2-pattern disappears and the pattern of subunit cell clusters remains when a higher threshold value of Mo-concentration is adopted for the projection contrast.

4. Conclusion

The HRTEM image of the short-range ordered Ni_4Mo was analyzed by using the IP system. The SRO state contains clusters of $D1_a$-, $D0_{22}$- and Pt_2Mo-type subunit cells. A mixed structure of the subunit cell clusters forms the projected pattern of N_2M_2-type which exhibits the {1 1/2 0} maxima in the diffraction pattern. It is clearly demonstrated that the digital processing of TEM image contrasts with the IP system enables us to analyze quantitatively local atomic structures in an SRO state.

Acknowledgements

We would like to thank Mr. T. Manabe of Kyushu University for his operation of the FETEM. This study was partly supported by Grant-in-Aid for Scientific Research (B) (2) (#08455293) from the Ministry of Education, Science, Sports and Culture, Japan.

References

1. G. Van Tendeloo, S. Amelinckx and D. de Fontaine, Acta crystallogr., **B41**, 281 (1985).
2. K. H. Lee, K. Hiraga, D. Shindo and M. Hirabayashi, Acta metall., **36**, 641 (1988).
3. M. Yamamoto, T. Hashizume and T. Sakurai, Scripta metall., **19**, 357 (1985).
4. M. Sundararaman, S. Banerjee and H. Wollenberger, Acta metall. mater., **43**, 107 (1995).
5. U. D. Kulkarni, S. Muralidhar and S. Banerjee, phys. stat. sol., **A110**, 331 (1988).
6. S. Hata, H. Fujita, S. Matsumura, N. Kuwano, K. Oki and D. Shindo, abstract 117th meeting of JIM in Honolulu, 96 (1995).
7. S. Hata, S. Matsumura, N. Kuwano and K. Oki, to be published.
8. D. Shindo, K. Hiraga, T. Oikawa and N. Mori, J. Electron Microscopy, **39**, 499 (1990).
9. D. Shindo, K. Hiraga, T. Oku and T. Oikawa, Ultramicroscopy, **39**, 50 (1991).
10. D. Shindo, T. Oku, J. Kudoh and T. Oikawa, Ultramicroscopy, **54**, 221 (1994).
11. P. De Meulenaere, D. Van Dyck, G. Van Tendeloo and J. Van Landuyt, Ultramicroscopy, **60**, 171 (1995).
12. P. De Meulenaere, G. Van Tendeloo, J. Van Landuyt and J. Van Dyck, Ultramicroscopy, **60**, 265 (1995).